

Pattern formation and transition in complex networks

Dongmei Song,¹ Yafeng Wang,¹ Xiang Gao,¹ Shi-Xian Qu,¹ Ying-Cheng Lai,^{2,3} and Xingang Wang^{1,*}

¹*School of Physics and Information Technology, Shaanxi Normal University, Xi'an 710062, China*

²*School of Electrical, Computer, and Energy Engineering,
Arizona State University, Tempe, Arizona 85287, USA*

³*Department of Physics, Arizona State University, Tempe, Arizona 85287, USA*

(Dated: April 3, 2017)

Dynamical patterns in complex networks of coupled oscillators are both of theoretical and practical interest, yet to fully reveal and understand the interplay between pattern emergence and network structure remains to be an outstanding problem. A fundamental issue is the effect of network structure on the stability of the patterns. We address this issue by using the setting where random links are systematically added to a regular lattice and focusing on the dynamical evolution of spiral wave patterns. As the network structure deviates more from the regular topology (so that it becomes increasingly more complex), the original stable spiral wave pattern can disappear and a different type of pattern can emerge. Our main findings are the following. (1) Short-distance links added to a small region containing the spiral tip can have a more significant effect on the wave pattern than long-distance connections. (2) As more random links are introduced into the network, distinct pattern transitions can occur, which include the transition of spiral wave to global synchronization, to a chimera-like state, and then to a pinned spiral wave. (3) Around the transitions the network dynamics is highly sensitive to small variations in the network structure in the sense that the addition of even a single link can change the pattern from one type to another. These findings provide insights into the pattern dynamics in complex networks, a problem that is relevant to many physical, chemical, and biological systems.

PACS numbers: 05.45.Xt, 89.75.Hc

I. INTRODUCTION

Pattern formation is ubiquitous in spatiotemporal dynamical systems in nature [1–3] ranging from granular materials [4] to ecosystems [5] and plants [6]. Complex dynamical networks, such as networks of coupled oscillators, are naturally spatiotemporal systems. The past two decades have witnessed a rapid growth of research on various types of dynamical processes in complex networks [7, 8], which include synchronization [9–18], virus spreading [19–26], traffic flow [27–33], and cascading failures [34–43]. In these studies, a primary issue was to address the interplay between the dynamical processes and the network structure. An interesting problem thus concerns pattern formation in complex networks, where a basic question is how the network structure affects the dynamical patterns. To our knowledge, in spite of the vast literature on dynamics in complex networks, a systematic study of the interplay between pattern formation and network structure is lacking. The purpose of this paper is to fill this knowledge gap by presenting results on pattern emergence, evolution, and transitions on networks undergoing systematic random structural perturbations.

To probe into the interplay between network structure and dynamical patterns in a concrete manner, we focus on coupled oscillator networks. An interesting phenomenon in such dynamical networks is that, under certain conditions, the oscillators can be self-organized to form spatial patterns [2]. As the formation of the patterns relies heavily on the symmetry of the coupling structure of the network, an intuitive thinking would suggest that it is unlikely for complex networks

to generate dynamical patterns [44, 45]. Yet, in natural and man-made systems, there are situations where well-organized patterns can form on complex networks, such as the firing patterns in the human brain [46]. A paradox was then how spatially ordered patterns can emerge from random or disordered coupling structures associated with a complex network. There have been previous efforts devoted to resolving this paradox. For example, pattern formation in complex network of coupled activators and inhibitors was studied, where Turing-like patterns were observed [47]. Complex networks of coupled excitable nodes were also studied [48] with respect to pattern formation in which the technique of dominant phase advanced driving was introduced, leading to the discovery of target-like wave patterns. Desynchronization patterns in complex network of coupled chaotic oscillators were subsequently studied [49], where it was found that reordering network nodes according to the eigenvector of the unstable mode can be effective at identifying the stable synchronous pattern from an asynchronous state. Recently, computational graph algorithms were introduced into the field of network synchronization to study synchronous patterns in large-size complex networks [50], where the important role of network symmetry in pattern formation was elucidated. In spite of the existing works, many questions concerning pattern formation and transition in complex networks remain, especially with respect to relatively more sophisticated patterns with complex spatial structures such as spiral waves [51].

The starting point of our study is then spiral waves in coupled oscillator networks, which are patterns observed ubiquitously in physical, chemical and biological systems [2]. Different from other types of patterns such as Turing patterns, the stability of a spiral wave depends crucially on the motion of the spiral tip [52, 53], leading to the specially designed meth-

* Email address: wangxg@snnu.edu.cn

ods for analyzing and controlling spiral waves [2]. In most previous works, spiral waves are studied for networks with a regular spatial structure, such as a periodic lattice. Nevertheless, there were works on spiral waves in systems with an irregular spatial structure [54–57]. For example, the formation of spiral waves in a medium possessing random (small-world) connections was studied [55] with the finding that, while the structural irregularity is detrimental to forming and sustaining a spiral wave, a small number of random links can counterintuitively enhance the wave stability. Another work [56] revealed that, random connections added locally to a regular medium can cause the meandering motion of the spiral tip to approach a fixed point. It was later found [57] that random connections introduced globally into a regular medium can lead to rich behaviors in the transition of the system dynamics among global synchronization state, steady state, and multiple spirals. These previous works indicated that the network structure can have a significant effect on pattern formation and transition, calling a systematic study of this issue.

To facilitate computation, we use coupled map lattices (CML) [58] to investigate the dynamical responses of spiral waves to structural perturbations. Historically, CMLs were used to understand patterns including spiral waves in complex media such as granular materials [59–61]. In our work, starting from a two-dimensional regular lattice capable of generating stable spiral waves, we systematically introduce random links into the network and study the transitions in the pattern dynamics as the network structure becomes increasingly random (complex). We uncover dynamical patterns and richer bifurcations that were not seen in previous works [55–57], such as chimera-like states where two synchronization clusters coexist with many asynchronous oscillators and the pinned multi-armed spirals in which the arms of the spiral are pinned to a square-shape boundary. An intriguing finding is that, in the region where pattern transitions occur, the dynamics is extremely sensitive to small changes in the network structure. These findings shed new lights on pattern behaviors in complex networks, which may lead to effective methods of pattern control.

In Sec. II, we introduce our CML system that is capable of generating spiral waves, and describe our strategy to supply random links. In Sec. III, we investigate pattern transitions as induced by a systematic change in the network structure, and present evidence of two types of patterns that have not been uncovered previously. In Sec. IV, we demonstrate the sensitivity of the patterns in the transition regions to small structural perturbations and elucidate the topological properties of the critical links. A discussion is presented in Sec. V.

II. MODEL AND METHOD

Network model. Our CML model with a general network structure reads [58, 62]

$$x_i(n+1) = (1-\varepsilon)f[x_i(n)] + \frac{\varepsilon}{k_i} \sum_{j=1}^N a_{ij}f[x_j(n)], \quad (1)$$

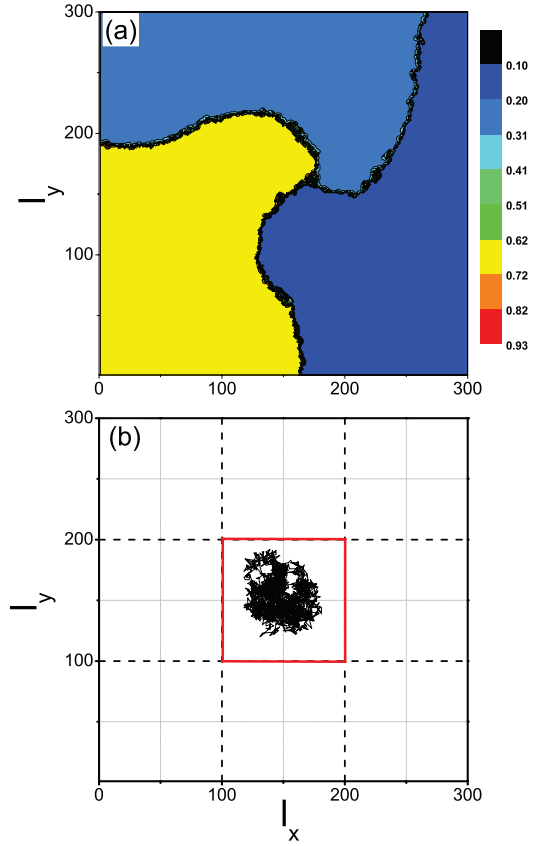


FIG. 1. (Color online) **An example of spiral wave in the regular lattice.** For $\varepsilon = 0.166$, a three-armed spiral wave generated by the system [Eqs. (1) and (2)]: (a) a snapshot of the system dynamics taken at $n = 3 \times 10^3$, (b) random motion of the spiral tip inside the central area marked by the (red) square.

with $i, j = 1, \dots, N$ are the nodal indices, N^2 is the system size, x_i is the state of the i th node at time n , and ε is the coupling parameter. The isolated dynamics of node i is governed by the nonlinear equation $x_i(n+1) = f[x_i(n)]$. The coupling structure of the system is characterized by the adjacency matrix A whose elements are given as: $a_{ij} = 1$ if nodes i and j are directly connected and $a_{ij} = 0$ otherwise. The degree of node i , the total number of links attached to it, is $k_i = \sum_j a_{ij}$.

Initially, the network is a two-dimensional regular lattice, where each interior node is coupled to its four nearest neighbors. We assume the free boundary condition and fix the system size to be 300×300 . The spatial location of a node in the network is (l_x, l_y) , where $1 \leq l_x, l_y \leq N$. For nodal dynamics, we adopt the piecewise linear map:

$$f(x) = \begin{cases} ax, & x < x_g, \\ b, & x \geq x_g, \end{cases} \quad (2)$$

where $x \in (0, 1)$, $x_g = 1/a$, a and b are independent parameters. Equation (2) is the discrete version of the differential Chay model used widely in computational neuroscience, and is capable of generating the similar bifurcation scenario of inter-spike interval (ISI) observed from experiments [63]. To be concrete, we fix $(a, b) = (2.5, 0.1)$, for which an iso-

lated node possesses a super-stable period-three orbit [64, 65]: $x_1^* = b \equiv A$, $x_2^* = ab \equiv B$, and $x_3^* = a^2b \equiv C$.

Generation of spiral waves. For a CML system, spiral waves can be stimulated through special initial conditions [62]. For example, we can choose the initial states of the nodes randomly within a narrow strip in the lattice, say $l_x \in [130, 170]$, with values uniformly distributed in the unit interval, while nodes outside the strip are set to have the initial value zero. For $\varepsilon = 0.166$, after a transient period of $n = 2.5 \times 10^3$ iterations, a stable three-armed spiral pattern is generated, as shown in Fig. 1(a), which is a snapshot of the system state. As the system evolves, the spiral arms rotate in a synchronous fashion and propagate outward from the tip. This feature of wave propagation is similar to that of spiral waves observed in other contexts, e.g., excitable media [2]. A close examination of the motion of the spiral tip reveals a difference: in an excitable medium the tip trajectory is often regular [66], but in our system it moves randomly inside the central region $100 < l_x, l_y < 200$, as shown in Fig. 1(b). In addition, in regions separated by the spiral arms, the nodes are synchronized into three distinct clusters, with nodes in each cluster being synchronized to the trajectory of a periodic point of the period-three orbit. The synchronous clusters have approximately the same size. The spiral arms themselves comprise asynchronous nodes, which constitute the cluster boundaries. We use the spiral pattern in Fig. 1(a) as the initial state and investigate the effect of randomly added links into the regular lattice.

Effect of adding random links on spiral wave patterns. As the dynamics of the spiral wave is slaved to the tip, applying random structural perturbations to the tip region can induce characteristic changes in the wave pattern [52, 53]. To gain insights, we first supply links between randomly chosen, unconnected pairs of nodes over the entire network [55–57]. The total number of such links is M , with the same coupling function and parameter as the regular links. For a fixed value of M , the network is initialized with the spiral wave pattern in Fig. 1(a) and the network state is recorded after 5×10^3 iterations. To characterize the deterioration of the perturbed spiral, we introduce the quantities $\rho_{max} = \max\{N_A, N_B, N_C\}/N^2$ and $\rho_{min} = \min\{N_A, N_B, N_C\}/N^2$, with N_A (N_B , N_C) being the number of nodes with state A (B, C), which represent, respectively, the normalized size of the largest and the smallest synchronous clusters associated with the spiral pattern. For the initial spiral [Fig. 1(a)], as the three clusters have approximately the same size, we have $\rho_{max} \approx \rho_{min} \approx 1/3$. If the sizes of the clusters are different, we have $\rho_{max} > 1/3$ and $0 < \rho_{min} < 1/3$, indicating a deformed but still sustained spiral. When a cluster disappears, we have $\rho_{min} \approx 0$, but the value of ρ_{max} may either be close to unity (if the system reaches global synchronization) or $1/2$ (if two equal-size clusters coexist). In this case, the original spiral has been destroyed. A simple criterion to determine the destruction of the spiral wave thus is $\rho_{min} \approx 0$. Figure 2(a) shows the variation of ρ_{min} with M (strategy 1). We see that, as M is increased from 0 to 150, ρ_{min} decreases from the value of about 0.27 to 0.05. Statistically, the spiral wave can sustain with less than 150 random links.

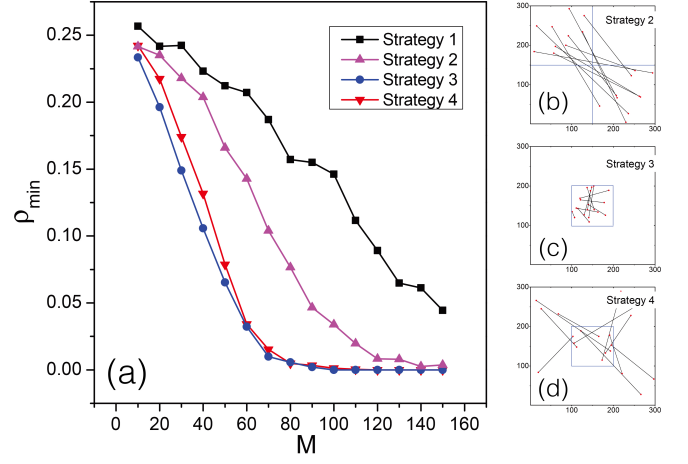


FIG. 2. (Color online) **Sustainability of spiral wave subject to different types of network structural perturbations.** (a) The variation in the normalized size of the smallest synchronous cluster, ρ_{min} , with M , the number of random links. Strategy 1: adding random links over the entire network (filled squares); Strategy 2: introducing long-distance random links (filled upper triangles); Strategy 3: supplying random links only in the central area (filled circles); Strategy 4: distributing random links between the central and peripheral regions (filled downward triangles). (b-d) Schematic illustrations of strategies 2, 3 and 4. Results in (a) are averaged over 200 network realizations.

In order to understand the role played by the spiral tip in the pattern stability, we study three alternative perturbation strategies [55–57]: introducing long-distance random links (Strategy 2), supplying random links only in the central area (Strategy 3), and distributing random links between the central and peripheral regions (Strategy 4). These three strategies are schematically illustrated in Figs. 2(b-d), respectively. For strategies 2 and 3, the pairs of nodes connected by the new links are randomly chosen from the regions $(0, 100) \times (200, 300)$ and $(200, 300) \times (0, 100)$ on the lattice, and from the central area $(100, 200) \times (100, 200)$, respectively. For strategy 4, one map is randomly chosen from the central area while another is chosen from the peripheral region. The results of applying perturbation strategies 2-4 are shown in Fig. 2(a), where we see that, strategies 3 and 4 are more effective at suppressing the spiral wave pattern than strategies 1 and 2. For example, the value of ρ_{min} is reduced to 0 at about $M = 140$ for strategy 2; while for strategies 3 and 4, this occurs at about $M = 100$. For the rest of the paper we focus on strategy 3.

III. PATTERN TRANSITIONS

To uncover and understand the pattern transitions as the network topology deviates from that of a regular lattice and becomes increasingly random, we calculate the variations of ρ_{max} and ρ_{min} with M (the total number of randomly added links according to perturbation strategy 3). As shown in Fig. 3, for a few randomly added links, say $M < 10$, we have

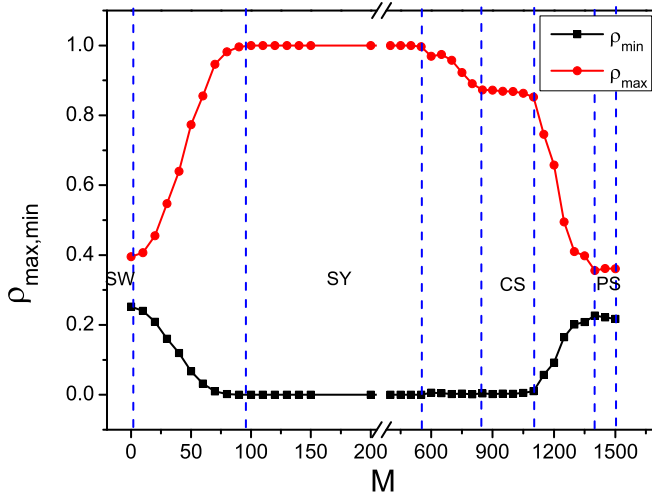


FIG. 3. (Color online) **Pattern transitions as the network structure becomes increasingly random.** Shown are ρ_{max} and ρ_{min} (the normalized sizes of the largest and the smallest synchronous cluster, respectively) versus M , the total number of randomly added links according to perturbation strategy 3. Spiral wave (SW) patterns exist in the parameter interval $M \in [0, 10]$. Global synchronization (SY) occurs for $M \in [100, 550]$. Chimera-like state (CS) arises in $M \in [850, 1100]$. For $M > 1400$, there is pinned spiral (PS). Ensemble average of 200 network realizations is used.

$\rho_{max} \approx \rho_{min} \approx 1/3$. In this region, the network exhibits a stable spiral wave similar to that in Fig. 1(a). As M is increased from 10, the value of ρ_{max} increases but ρ_{min} decreases. For $M \approx 100$, we have $\rho_{max} = 1$ and $\rho_{min} = 0$, signifying that the network has reached a uniform synchronization state without any spatial pattern. Figure 4(a) shows, for $M = 100$, with time the spiral tip shifts from the central to the peripheral area [Fig. 4(a2)]. The spiral tip vanishes when it reaches the lattice boundary. Subsequently, one of the synchronous clusters expands while the other two clusters are pushed toward the boundary, leading finally to the state of global synchronization, as shown in Fig. 4(a3).

Figure 3 indicates that the global synchronization state is stable for $M \lesssim 550$. As M is increased further, ρ_{max} decreases gradually but the value of ρ_{min} remains about 0. For $M \approx 850$, another platform emerges in the variation of ρ_{max} with M , where $\rho_{max} \approx 0.9$ for $M \in [850, 1100]$. Since $\rho_{min} \approx 0$ still holds, there is no spiral wave. In fact, in this region the system contains at most two synchronous clusters. Because the value of ρ_{max} is close to unity, most nodes in the network are synchronized into a giant cluster. To provide evidence for this scenario, we calculate a series of snapshots of the system dynamics for $M = 1000$, which are shown in Fig. 4(b). We see that, the original spiral wave first breaks into a pair of anti-spiral waves [Fig. 4(b2)] that move gradually to the system boundary and disappear after reaching it. In the meantime, two synchronous clusters emerge: a small cluster consisting of nodes in the central area (except for the nodes connected by the randomly added links) and a large cluster comprising nodes in the peripheral area. There is a narrow boundary of asynchronous nodes separating the two clusters,

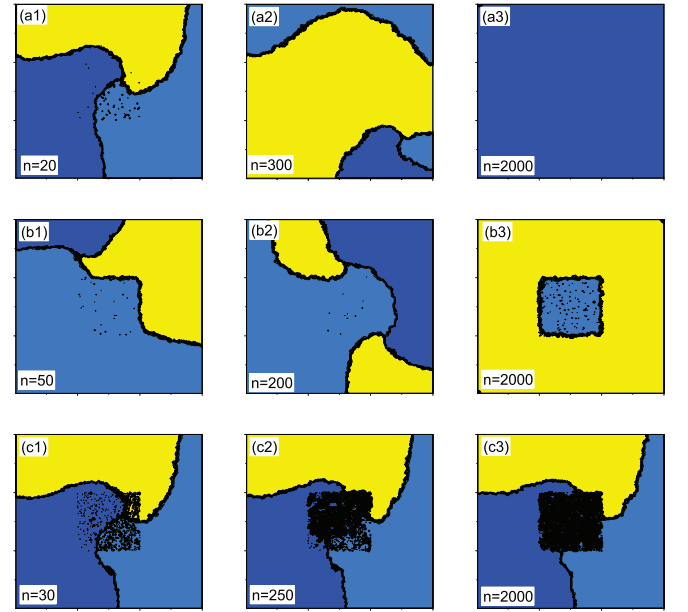


FIG. 4. (Color online) **Characteristically distinct dynamical states in the network system that structurally becomes increasingly random** for (a1-a3) $M = 100$ (global synchronization) (b1-b3) $M = 1000$ (chimera-like state) and (c1-c3) $M = 1500$ (pinned spiral wave). The left, middle and right columns are snapshots of the system dynamics taken, respectively, at the initial, middle and end of the evolution. Black dots in the central area mark the ending nodes of the randomly added links.

as shown in Fig. 4(b3). The distinct synchronous clusters represent effectively a chimera state observed previously in systems of non-locally coupled oscillators [67–70], which becomes unstable as M is increased through 1100, since ρ_{max} and ρ_{min} tend to decrease and increase, respectively. For $M \gtrsim 1400$, the values of ρ_{max} and ρ_{min} are stabilized about $1/3$ and $1/4$, respectively. Figure 4(c) shows, for $M = 1400$, the typical states emerged during the system evolution. Due to the added random links, the spiral tip first drifts from the central to the peripheral area [Fig. 4(c1)], but the drift stops at the boundary of the central area after which the tip disappears. During this time interval, the spiral arms are separated from each other. As will be demonstrated below, the three arms are attached to the boundary of the central area and rotate in a synchronous fashion, signifying the phenomenon of pinned spirals [71]. As M is increased further, the pinned spiral state can be maintained (even for $M = 1 \times 10^4$).

Figures 3 and 4 suggest the following transition scenario as more random links are added to the network: spiral wave \rightarrow global synchronization \rightarrow chimera-like state \rightarrow pinned spiral wave, where each state exists in a finite parameter region. Within each region, the values of ρ_{max} and ρ_{min} are hardly changed, suggesting that the respective patterns are stable to random structural perturbations. A transition region is associated with dramatic changes in the value of ρ_{max} or ρ_{min} , in which one type of pattern is destroyed and a new type is born. To better characterize the transition regions, we calculate the probability of certain pattern, p_{state} , as a function of

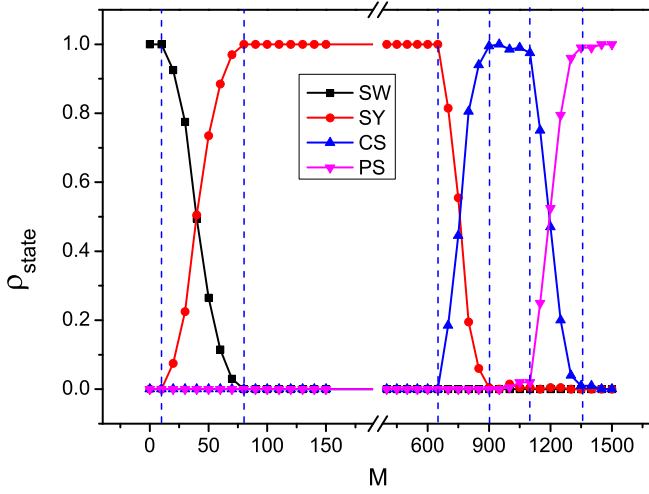


FIG. 5. (Color online) **Continuous nature of pattern transition.** Shown is p_{state} versus M , which denotes the probability of generating a specific pattern for M randomly added links. The terms SW, SY, CS and PS stand for, respectively, spiral wave, global synchronization, chimera-like state, and pinned spiral wave. Results are averaged over 200 network realizations.

M . The results are shown in Fig. 5. Comparing Figs. 3 and 5, we see that two different patterns coexist in each transition region. Taking $M = 30$ as an example, we see that, over 200 independent network realizations, about 80% of these lead to a spiral wave ($p_{\text{sp}} \approx 0.8$) whereas the remaining cases correspond to the global synchronization state ($p_{\text{gs}} \approx 0.2$). In the transition region between spiral wave and global synchronization ($10 < M < 100$), p_{sp} decreases from unity to zero, which is accompanied by an increase in p_{gs} in the opposite direction. This feature of gradual and continuous transition appears also in other transition regions, as shown in Fig. 5.

IV. PATTERN SENSITIVITY IN THE TRANSITION REGIONS

In the transition regions the system dynamics is sensitive to random structural perturbations in the sense that a single added random link is able to switch the system dynamics from one pattern to another. For example, for a network with $M = 49$ random links, the stable state of the system is a spiral wave pattern. With a new random link, the state of global synchronization emerges and becomes stable, as exemplified in Figs. 6(a-d), where the time evolutions of different pattern states, $\delta \mathbf{X} = \mathbf{X}_{M=49} - \mathbf{X}_{M=50}$, are shown, with $\mathbf{X}_M = \{x_i\}$ denoting the pattern state for the network with M random links. Initially [Fig. 6(a)], except for the pair of nodes connected by the 50th link, the two patterns are essentially identical as the two networks (one with 49 and another with 50 random links) start from the same initial condition [the spiral wave in Fig. 1(a)]. Then, as the two system evolves, the difference at one of the ending node of the 50th link is disappeared, whereas the difference of the other ending node is kept and gradually propagated to its neighboring region [Fig. 6(b)]. At

a later time the difference switches to a remote ending node of a random link in the lattice [Fig. 6(c)]. This propagation and switching process occurs repeatedly in the central area, resulting in the formation of a three-armed spiral, as shown in Fig. 6(d). Finally, a spiral wave similar to that in Fig. 1 is generated. Similar behaviors arise in other transitional regions [$M \in (550, 850)$ and $M \in (1100, 1400)$].

Do the critical connections possess any special topological property? To address this question, in the first transition region, we add the 50th link in the central area randomly. If the system evolves finally into the state of global synchronization, we mark this link as critical and record the locations of the ending nodes, denoted by (l_x, l_y) and (l'_x, l'_y) . For comparison, we also record the ending nodes of non-critical links that do not lead to the destruction of the spiral wave. We first examine the Euclidean distances of the critical links, defined as $d = [(l_x - l'_x)^2 + (l_y - l'_y)^2]^{1/2}$. Previous studies [72, 73] revealed that long distance links have a more significant effect on the network dynamics than short range links. A higher probability for a critical link to be long ranged can then be intuitively expected. Figure 6(e) shows the normalized distribution of the distances of the critical links. Surprisingly, the distribution is unimodal with the maximum probability occurring at about $d = 50$. For comparison, the distance distribution of the non-critical is also shown, where we see that the two distributions are nearly identical. This analysis indicates that the critical links are uncorrelated with the distance.

The local connectivity of the ending nodes associated with the critical links represents another topological feature. To examine it, for each ending node, we count the number n_r of nodes of degree larger than 4 within the distance $d_r = 10$ from it, for the reason that there is at least one random link attached to such a node. If the critical links were attached to the existing nodes following the preferential attachment rule, such links would be more likely to lie in regions containing large degree nodes. In this case, the distribution of n_r should exhibit a heavy tail. A representative distribution of k_r , the sum of the critical links of the ending nodes, is shown in Fig. 6(f), which exhibits a unimodal feature. For comparison, the k_r distribution of the non-critical links is also shown, which is indistinguishable from that associated with critical links. We find that the distance d_r has no effect on the unimodal feature. The results thus suggest that local connectivity is uncorrelated with the critical links.

Examination of additional topological properties [7] such as the degree assortativity, network modularity, and average network diameter revealed no clear difference between the critical and non-critical links. Topological analyses have also been carried out for other transition regions, with the results essentially the same. Our conclusion is that there is little difference between the critical and non-critical links.

V. DISCUSSION

In a regular lattice of coupled nonlinear oscillators, a typical (or default) pattern is spiral wave. A sufficient number of random links will destroy the spiral wave, but how? This pa-

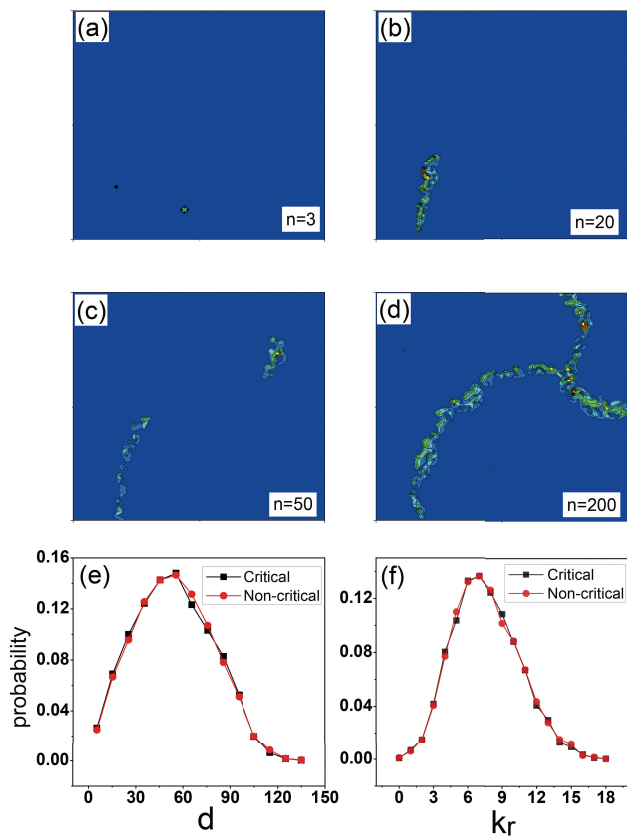


FIG. 6. (Color online) **Pattern sensitivity in the transition regions.** (a-d) Time evolution of the difference δX between the spiral wave ($M = 49$) and the global synchronization state ($M = 50$). (e) Normalized distance distribution of the critical (filled squares) and non-critical links (filled circles). (f) Normalized distribution of the local connectivity of the critical (filled squares) and non-critical links (filled circles). Results in (e) and (f) are averaged over 500 realizations of the 50th link.

per addresses this question through a detailed computational study of the effect of random links on a dynamical pattern as their number is systematically increased. From the point of view of network structure, adding random links to a regular network makes it complex, thus our work effectively addresses the general problem of pattern formation and transition in complex networks. We find, as the number of randomly added links is increased, the underlying networked system can exhibit distinct types of dynamical patterns and rich transitions among them. Our study has revealed two types of pat-

terns in complex networks, which to our knowledge have not been reported previously: a chimera-like pattern and pinned multi-armed spiral waves. We also find that a transition between two distinct types of patterns can be triggered through only a single, critical random link. The topological properties of the set of critical links are found to be no different from those of the non-critical links. With respect to spiral waves, our study reveals that random links added into the region of the spiral tip can have a devastating effect on the pattern, a result that is consistent with those from previous works [55–57].

A key difference from previous studies is that in our system the motion of the spiral tip is random in a limited area (the central area), which leads to the sensitivity of the system pattern in the transition regions. This has a consequence. In particular, a previous result in the study of synchronization transitions in complex networks was that, as the network becomes increasingly complex, an order parameter characterizing the degree of network synchronization can increase continuously [74]. As demonstrated in this work, for spiral wave patterns a properly defined order parameter would exhibit a non-monotonous behavior because, as the number of random links is increased, the state of the network can become perfectly ordered (global synchronization) and then become less ordered with a chimera-like state and a pinned multi-armed spiral. This peculiar phenomenon may be specific to spiral-wave patterns where we supply random links only to the tip region. Indeed, when random links are added to the network on a global scale (as with the Newman-Watts small-world network model [75]), we find a monotonic change in the degree of the order of the system state. Nonetheless, our study sheds new lights on the pattern dynamics in complex networks and our results provide insights into the issue of pattern control on networks.

ACKNOWLEDGEMENTS

We thank Prof. H. Zhang for helpful discussions. This work was supported by the National Natural Science Foundation of China under the Grant No. 11375109 and by the Fundamental Research Funds for the Central Universities under the Grant No. GK201601001. YCL would like to acknowledge support from the Vannevar Bush Faculty Fellowship program sponsored by the Basic Research Office of the Assistant Secretary of Defense for Research and Engineering and funded by the Office of Naval Research through Grant No. N00014-16-1-2828.

- [1] M. C. Cross and P. C. Hohenberg, Rev. Mod. Phys. **65**, 851 (1993).
- [2] M. Cross and H. Greenside, *Pattern Formation and Dynamics in Nonequilibrium Systems*, 1st ed. (Cambridge University Press, 2010).
- [3] R. Hoyle, *Pattern Formation - An Introduction to Methods*, 1st ed. (Cambridge University Press, 2006).

- [4] I. S. Aranson and L. S. Tsimring, Rev. Mod. Phys. **78**, 641 (2006).
- [5] M. Rietkerk and J. van de Koppel, Trends Ecol. Evol. **23**, 169 (2008).
- [6] V. Willemsen and B. Scheres, Ann. Rev. Genetics **38**, 587 (2004).

- [7] M. E. J. Newman, *Networks: An Introduction* (Oxford University Press, 2010).
- [8] A. Barrat, M. Barthélemy, and A. Vespignani, *Dynamical Processes on Complex Networks* (Harvard University Press, Cambridge, MA, 2008).
- [9] L. F. Lago-Fernandez, R. Huerta, F. Corbacho, and J. A. Siguenza, Phys. Rev. Lett. **84**, 2758 (2000).
- [10] P. M. Gade and C.-K. Hu, Phys. Rev. E **62**, 6409 (2000).
- [11] J. Jost and M. P. Joy, Phys. Rev. E **65**, 016201 (2001).
- [12] M. Barahona and L. M. Pecora, Phys. Rev. Lett. **89**, 054101 (2002).
- [13] V. Belykh, I. Belykh, and M. Hasler, Physica D **195**, 159 (2004).
- [14] M. Chavez, D.-U. Hwang, A. Amann, H. G. E. Hentschel, and S. Boccaletti, Phys. Rev. Lett. **94**, 218701 (2005).
- [15] C. Zhou and J. Kurths, Phys. Rev. Lett. **96**, 164102 (2006).
- [16] L. Huang, K. Park, Y.-C. Lai, L. Yang, and K. Yang, Phys. Rev. Lett. **97**, 164101 (2006).
- [17] X. G. Wang, L. Huang, Y.-C. Lai, and C.-H. Lai, Phys. Rev. E **76**, 056113 (2007).
- [18] S.-G. Guan, X. G. Wang, Y.-C. Lai, and C. H. Lai, Phys. Rev. E **77**, 046211 (2008).
- [19] R. Pastor-Satorras and A. Vespignani, Phys. Rev. Lett. **86**, 3200 (2001).
- [20] K. T. D. Eames and M. J. Keeling, Proc. Natl. Acad. Sci. (USA) **99**, 13330 (2002).
- [21] D. J. Watts, R. Muhamad, D. C. Medina, and P. S. Dodds, Proc. Natl. Acad. Sci. (USA) **102**, 11157 (2005).
- [22] V. Colizza, A. Barrat, M. Barthélemy, and A. Vespignani, Proc. Natl. Acad. Sci. (USA) **103**, 2015 (2006).
- [23] J. Gómez-Gardeñes, V. Latora, Y. Moreno, and E. Profumo, Proc. Natl. Acad. Sci. (USA) **105**, 1399 (2008).
- [24] P. Wang, M. C. González, C. A. Hidalgo, and A.-L. Barabási, Science **324**, 1071 (2009).
- [25] S. Merler and M. Ajelli, Proc. Roy. Soc. B Bio. Sci. **277**, 557 (2010).
- [26] D. Balcan and A. Vespignani, Nat. Phys. **7**, 581 (2011).
- [27] A. Arenas, A. Díaz-Guilera, and R. Guimerà, Phys. Rev. Lett. **86**, 3196 (2001).
- [28] P. Echenique, J. Gómez-Gardeñes, and Y. Moreno, Phys. Rev. E **70**, 056105 (2004).
- [29] L. Zhao, Y.-C. Lai, K. Park, and N. Ye, Phys. Rev. E **71**, 026125 (2005).
- [30] X. G. Wang, Y.-C. Lai, and C.-H. Lai, Phys. Rev. E **74**, 066104 (2006).
- [31] S. Meloni, J. Gómez-Gardeñes, V. Latora, and Y. Moreno, Phys. Rev. Lett. **100**, 208701 (2008).
- [32] H.-X. Yang, W.-X. Wang, Y.-B. Xie, Y.-C. Lai, and B.-H. Wang, Phys. Rev. E **83**, 016102 (2011).
- [33] R. G. Morris and M. Barthelemy, Phys. Rev. Lett. **109**, 128703 (2012).
- [34] A. E. Motter and Y.-C. Lai, Phys. Rev. E **66**, 065102(R) (2002).
- [35] L. Zhao, K. Park, and Y.-C. Lai, Phys. Rev. E **70**, 035101(R) (2004).
- [36] A. Galstyan and P. Cohen, Phys. Rev. E **75**, 036109 (2007).
- [37] J. P. Gleeson, Phys. Rev. E **77**, 046117 (2008).
- [38] L. Huang, Y.-C. Lai, and G. Chen, Phys. Rev. E **78**, 036116 (2008).
- [39] R. Yang, W.-X. Wang, Y.-C. Lai, and G. Chen, Phys. Rev. E **79**, 026112 (2009).
- [40] S. V. Buldyrev, R. Parshani, G. Paul, H. E. Stanley, and S. Havlin, Nature (London) **464**, 1025 (2010).
- [41] R. Parshani, S. V. Buldyrev, and S. Havlin, Phys. Rev. Lett. **105**, 048701 (2010).
- [42] R. Parshani, S. V. Buldyrev, and S. Havlin, Proc. Natl. Acad. Sci. (USA) **108**, 10071010 (2011).
- [43] R.-R. Liu, W.-X. Wang, Y.-C. Lai, and B.-H. Wang, Phys. Rev. E **85**, 026110 (2012).
- [44] K. Park, L. Huang, and Y.-C. Lai, Phys. Rev. E **75**, 026211 (2007).
- [45] X. G. Wang, S.-G. Guan, Y.-C. Lai, B.-W. Li, and C.-H. Lai, Europhys. Lett. **88**, 28001 (2009).
- [46] E. Basar, *Brain Function and Oscillation* (Springer, New York, 1998).
- [47] H. Nakao and A. S. Mikhailov, Nat. Phys. **6**, 544 (2010).
- [48] Y. Qian, X. Huang, G. Hu, and X. Liao, Phys. Rev. E **81**, 036101 (2010).
- [49] C. Fu, H. Zhang, M. Zhan, and X. G. Wang, Phys. Rev. E **85**, 066208 (2012).
- [50] L. M. Pecora, F. Sorrentino, A. M. Hagerstrom, T. E. Murphy, and R. Roy, Nat. Commun. **5**, 4079 (2014).
- [51] M.-T. Huett, M. Kaiser, and C. C. Hilgetag, Philos. Trans. Roy. Soc. B **369**, 20130522 (2014).
- [52] D. Barkley, Phys. Rev. Lett. **72**, 164 (1994).
- [53] H. Guo, H. Liao, and Q. Ouyang, Phys. Rev. E **66**, 026104 (2002).
- [54] A. V. Panfilov, Phys. Rev. Lett. **88**, 118101 (2002).
- [55] D. He, G. Hu, M. Zhan, W. Ren, and Z. Gao, Phys. Rev. E **65**, 055204 (2002).
- [56] X. Wang, Y. Lu, M. Jiang, and Q. Ouyang, Phys. Rev. E **69**, 056223 (2004).
- [57] S. Sinha, J. Saramäki, and K. Kaski, Phys. Rev. E **76**, 015101 (2007).
- [58] K. Kaneko, *Theory and Application of Coupled Map Lattices* (Wiley, Chichester, 1993).
- [59] S. C. Venkataramani and E. Ott, Phys. Rev. Lett. **80**, 3495 (1998).
- [60] S. C. Venkataramani and E. Ott, Phys. Rev. E **63**, 046202 (2001).
- [61] M. A. F. Harrison and Y.-C. Lai, Int. J. Bif. Chaos **18**, 1627 (2008).
- [62] R. Kapral, R. Livi, G.-L. Oppo, and A. Politi, Phys. Rev. E **49**, 2009 (1994).
- [63] J. Mo, Y. Li, C. Wei, M. Yang, H. Gu, S. Qu, and W. Ren, Chin. Phys. B **19**, 080513 (2010).
- [64] S.-X. Qu, S. Wu, and D.-R. He, Phys. Rev. E **57**, 402 (1998).
- [65] K. Yang, X. G. Wang, and S.-X. Qu, Phys. Rev. E **92**, 022905 (2015).
- [66] G. Li, Q. Ouyang, V. Petrov, and H. L. Swinney, Phys. Rev. Lett. **77**, 2105 (1996).
- [67] Y. Kuramoto and D. Battogtokh, Nonlin. Phen. Complex Syst. **5**, 380 (2002).
- [68] D. M. Abrams and S. H. Strogatz, Phys. Rev. Lett. **93**, 174102 (2004).
- [69] N. Yao, Z.-G. Huang, Y.-C. Lai, and Z.-G. Zheng, Sci. Rep. **3**, 3522 (2013).
- [70] N. Yao, Z.-G. Huang, C. Grebogi, and Y.-C. Lai, Sci. Rep. **5**, 12988 (2015).
- [71] D. Pan, X. Gao, X. Feng, J. Pan, and H. Zhang, Sci. Rep. **6**, 21876 (2012).
- [72] Y. Qian, Chin. Phys. B **21**, 088201 (2012).
- [73] K. Xu, W. Huang, B. Li, M. Dhamala, and Z. Liu, Europhys. Lett. **102**, 50002 (2013).
- [74] A. Arenas, A. Diaz-Guilera, J. Kurths, Y. Moreno, and C. S. Zhou, Phys. Rep. **469**, 93 (2008).
- [75] M. E. J. Newman and D. J. Watts, Phys. Lett. A **263**, 341 (1999).